

**NASA TECHNICAL
MEMORANDUM**

NASA TM X-73643

NASA TM X-73643

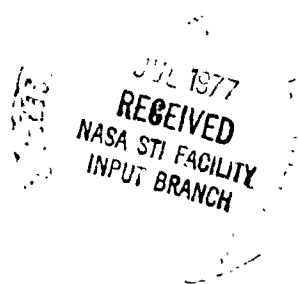
(NASA-TM-X-73643) SOLAR ARRAY MAXIMUM POWER
TRACKING WITH CLOSED-LOOP CONTROL OF A
30-CENTIMETER ION THRUSTER (NASA) 25 P HC
A02/MF A01 CSCL 21C

N77-26222

G3/20 Unclas
31869

SOLAR ARRAY MAXIMUM POWER TRACKING WITH CLOSED-
LOOP CONTROL OF A 30-CENTIMETER ION THRUSTER

by R. P. Gruber
Lewis Research Center
Cleveland, Ohio 44135
March 1977



1 Report No NASA TM X-73643	2 Government Accession No.	3 Recipient's Catalog No.
4 Title and Subtitle SOLAR ARRAY MAXIMUM POWER TRACKING WITH CLOSED- LOOP CONTROL OF A 30-CENTIMETER ION THRUSTER		5 Report Date
7 Author(s) R. P. Gruber		6 Performing Organization Code
9 Performing Organization Name and Address Lewis Research Center National Aeronautics and Space Administration Cleveland, Ohio 44135		8 Performing Organization Report No E-9148
12 Sponsoring Agency Name and Address National Aeronautics and Space Administration Washington, D.C. 20546		10 Work Unit No.
		11 Contract or Grant No.
		13 Type of Report and Period Covered Technical Memorandum
		14 Sponsoring Agency Code
15 Supplementary Notes		
16. Abstract A new solar array/ion thruster system control concept has been developed and demonstrated. An ion thruster beam load is used to automatically and continuously operate an unregulated solar array at its maximum power point independent of variations in solar array voltage and current. Preliminary tests were run which verified that this method of control can be implemented with a few, physically small, signal level components dissipating less than two watts.		
17 Key Words (Suggested by Author(s)) Maximum power tracking Solar array		18 Distribution Statement Unclassified - unlimited
19 Security Classif (of this report) Unclassified	20 Security Classif (of this page) Unclassified	21 No. of Pages
		22 Price*

**SOLAR ARRAY MAXIMUM POWER TRACKING WITH CLOSED-
LOOP CONTROL OF A 30-CENTIMETER ION THRUSTER**

by R. P. Gruber

Lewis Research Center

SUMMARY

E-9148

A new control concept for solar array/ion thruster systems has been developed and demonstrated that uses the thruster itself to operate an unregulated solar array at the maximum power point. The thruster beam current is adjusted under closed loop control so that the solar array always operates at the maximum power point independent of variations in the solar intensity or array temperature. System tests were run and have verified that no fundamental problems exist for this method of control. This control technique could minimize the mass-to-power ratio of a solar electric propulsion system. In addition, since an unregulated solar array is used, system hardware is simplified. However, mission analysis becomes more complex, since specific impulse and thrust vary as a function of solar array voltage and current. Preliminary tests have demonstrated that this control method can be implemented using a few physically small signal level components.

INTRODUCTION

The application of electron-bombardment ion thruster systems has been analyzed in detail for a broad set of planetary (refs. 1 to 4) and near earth (refs. 5 to 7) missions. The thrust systems assumed for contemporary studies employed the 30-cm diameter mercury bombardment ion thruster (ref. 8) presently under development by the Lewis Research Center.

As discussed in the referenced mission studies, ion thrusters are typically powered by solar arrays used in conjunction with power processing equipment. The power processing equipment matches the thruster

load requirements to the solar array. For the high power, high voltage levels encountered with thruster loads, power processors are heavy, complex, expensive and are a substantial burden to the spacecraft thermal control system. Considerable efforts are being made to develop alternate power processing concepts to reduce these spacecraft penalties.

One of the alternate concepts under consideration is the Integrally Regulated Solar Array (IRSA). The IRSA system provides regulated dc power from a controlled solar array directly to its loads without an intervening power processor (refs. 9 and 10). An integrally regulated solar array was used to power a 30-cm ion thruster beam load (ref. 11). It was determined from this effort that the basic characteristics of solar arrays (such as ripple and inherent current limited output) were well matched to thruster requirements. Integrally regulated solar arrays typically comprise blocks of cells that are automatically switched in or out by closed loop control to provide voltage or current regulation. When this method of regulation is used, the cells that are switched out become dead weight, resulting in a higher subsystem mass to power ratio. Minimization of the solar electric propulsion system mass to power ratio is clearly of primary importance so it is desirable that all available solar array power be used. Therefore it is highly desirable to operate the solar array at the maximum power point under all conditions of operation.

Systems capable of operating a solar array at its maximum power point have been demonstrated (refs. 12 to 14). However, these systems incorporate batteries for energy storage. Presently conceived solar electric propulsion systems do not use batteries to augment beam power because of the added weight. For most systems without batteries, dynamics considerations make an automatic maximum power point tracker more difficult to implement.

Methods of maintaining a solar array at its maximum power point fall into two categories: (1) open loop and (2) closed loop. Open loop systems measure one or more array parameters and then predict or determine the array maximum power point. A system using this technique could include a small reference array. Closed loop techniques determine the location

of the maximum power point directly and maintain the system at that point. With open loop techniques it is generally not practicable to accommodate unpredictable changes in solar array output. (such as those caused by severely degraded cells). Closed loop techniques considered to date by others (ref. 15) for ion thruster systems have been limited in performance because of systems dynamics constraints and power dissipation.

A new technique for solar array/ion thruster systems has been developed and demonstrated that uses the thruster itself to operate an unregulated solar array at the maximum power point. The thruster beam current is adjusted under closed loop control so that the solar array always operates at the maximum power point. The maximum power point location is determined by using the thruster to slightly perturb the array and thus obtain very small changes in array power.

The small power changes are then used to determine the location of the array maximum power point in relation to the actual operating point. The thruster beam current is then automatically adjusted until the following array condition is satisfied:

$$dP_A = \left(\frac{\partial P_A}{\partial I_A} \right) dI_A + \left(\frac{\partial P_A}{\partial V_A} \right) dV_A = 0$$

As a result of direct coupling to an unregulated solar array, the thruster voltage and current at the maximum power point vary with array temperature, incident light and array degradation. System specific impulse varies approximately as:

$$I_{sp} \text{ (sec)} \cong 100 \sqrt{V_A}$$

and thrust varies approximately as:

$$T \text{ (mN)} \cong 2.039 I_A \sqrt{V_A}$$

where V_A is array volts and I_A is array amperes.

For some mission sets, the array voltage change will be small, for others it may change markedly. Since mission studies to date have not considered continuously varying specific impulse and thrust, new analysis will need to be accomplished to characterize systems incorporating this method of maximum power tracking.

The concept development and preliminary demonstration reported herein provides information that can be used for solar array/ion thruster system development.

SYSTEM TEST EQUIPMENT

A 30-cm diameter electron bombardment mercury ion thruster, one unregulated solar array, a conventional power processor and specially developed maximum power tracking control circuits were used for this thruster system test. Figure 1 shows a functional diagram of the test configuration. The system is arranged so that the thruster can be initially operated exclusively from the power processor. Switches are used to replace the power processor beam supply with the solar array and to replace the fixed beam current reference with the power tracker beam current reference.

Thruster

The ion thruster provides thrust by generating, accelerating, and expelling a beam of mercury ions. The energetic ions leaving the thruster are space charge neutralized by electrons from a neutralizer. Basically, liquid mercury is vaporized to provide a controlled propellant flow of mercury atoms into discharge chamber. Ionization occurs when an atom loses an electron after bombardment by a (40 eV) discharge chamber electron. The electrons and the ions form a plasma in the ionization chamber. An electric field between a screen and an accelerator grid draws ions from the plasma and accelerates them out through many small holes in the grid set to form an ion beam. A neutralizer injects an equal number of electrons into the ion beam.

The ion thruster electrical load requiring the most power is the ion beam load. This plasma load typically consumes about 3/4 of the total thruster power at full throttle. The power supplied to the beam is approximately related to thrust as:

$$T(\text{mN}) \cong 2.039 I_B \sqrt{V_B}$$

and to specific impulse approximately as:

$$I_{\text{sp}} (\text{sec}) \cong 100 \sqrt{V_B}$$

Where I_B is the beam current and V_B is the beam voltage.

The beam current is controlled by varying the number of neutral mercury atoms flowing to the discharge. The flow rate is determined by the temperature of the porous vaporizer which is controlled by a vaporizer heater.

A 30-cm diameter mercury bombardment ion thruster (No. 501) was used for this test. This "400 series" thruster was originally built by Hughes Research Laboratories and was modified at NASA-Lewis to be essentially equivalent to a 700 series Engineering Model Thruster (EMT) described in reference 16. These modifications included the neutralizer assembly, dished grids of the EMT geometry, "800 series" main- and cathode-isolator-vaporizers, an increased magnetic field and a $10\frac{1}{2}$ turn magnetic baffle. Both cathode and neutralizer had 900 series impregnated inserts.

Solar Array

A 700 volt open circuit, 1.2 A short circuit solar array chosen for convenience was assembled from 5 modules in the 1 kilowatt laboratory solar array facility described in reference 17. The facility consists of 9 independent modules, each of which contains an array of 2560 solar cells (2- by 2-cm), a tungsten-iodide lamp bank, infrared filter, and water and air cooling for the cells and lamps respectively. Each module array con-

tains two subpanels of 40 series strings which are 32 solar cells long. Figure 2 shows one of the modules opened to display the solar array and its lamp bank. Depending on the internal wiring, each module can produce approximately 120 watts at voltages from 12 volts to 1.2 kilovolts. The modules can be interconnected in any series-parallel arrangement.

Conventional Power Processors

The transistor bridge converter test console described in reference 18 was used for this test. Although this unit is a laboratory test console, it incorporates all the controls necessary for closed-loop thruster operation and is functionally representative of a flight type power processor. The converters supplying the accelerator and discharge load operate at a switching frequency of approximately 10 kHz. The converters supplying the remaining thruster loads operate at 5 kHz. In order to use the thruster beam current controller to track maximum array power, the fixed beam current reference voltage was simply replaced by the maximum power tracking control circuit output reference.

Maximum Power Tracking Control Circuits

A functional diagram of the solar array/ion thruster maximum power tracker control circuit is shown in figure 3. The Appendix discusses the circuit in detail. Circuit functions are described as follows: Solar array voltage and current are continuously measured to determine array power. The circuit constantly changes the beam current reference to maintain operation at the maximum power point. The frequency of the array current changes is adjustable. For the tests reported herein the frequencies were 0.030 Hz and 0.037 Hz. Power is maximized when the first derivative of power with respect to current is equal to zero. During this time the array voltage-current characteristic must be virtually constant. The circuit generates the first derivative of power with respect to time by varying array current. However setting dP/dt equal to zero is shown to be equivalent to setting dP/dI equal to zero by the following:

$$\frac{dP}{dt} = \left(\frac{\partial P}{\partial I_A} \right) \frac{dI_A}{dt} + \left(\frac{\partial P}{\partial V_A} \right) \frac{dV_A}{dt} = 0$$

and

$$\frac{dV_A}{dt} = \frac{dV_A}{dI_A} \times \frac{dI_A}{dt}$$

so,

$$dP = \left(\frac{\partial P}{\partial I_A} \right) dI_A + \left(\frac{\partial P}{\partial V_A} \right) \left(\frac{dV_A}{dI_A} \right) dI_A = 0$$

Therefore,

$$\frac{dP}{dI} = \left(\frac{\partial P}{\partial I_A} \right) + \left(\frac{\partial P}{\partial V_A} \right) \left(\frac{dV_A}{dI_A} \right) = 0$$

In order to be able to obtain the first derivative of power with respect to time, the thruster beam current is perturbed of order 5 percent peak to peak with a clock and associated ramp generator. The amount of current perturbation is adjustable. (Perturbation current amplitude not optimized for tests reported herein.) Array power, the first derivative of array power and array current changes are then all phase related to the clock.

The phase of the first derivative relative to the clock is determined by the location of the thruster beam current operating point on the array characteristic. If the first derivative of power is positive with increasing current (operating point on the low current side of the maximum power point) it is in phase with the clock. If the first derivative of power is negative with increasing current (operating point on the high current side of the maximum power point) it is out of phase with the clock by 180°. When the operating point is on the maximum power point the first derivative of power averages zero. The circuits used to determine the phase relationship between the first derivative of array power and the clock for positive, negative or zero

first derivative are the zero crossing detector, shaping circuit and phase demodulator. The zero crossing detector and shaping circuit provide a square pulse in or out of phase with the clock according to whether the sign of the first derivative of power is either positive or negative respectively. The phase demodulator output is positive for in phase, negative for out of phase and averages zero at the maximum power point. When the operating point is at the maximum power point, the first derivative of power changes sign twice for each half cycle of the clock. This results in an average output of zero from the phase demodulator. The integrator input is then averaging zero, so integrator output does not change. In this maximum power condition the array/thruster operating point is not changed. When the operating point is not at the maximum power point, the phase demodulator output drives the integrator and beam current reference towards the maximum power point.

EXPERIMENTAL PROCEDURE

Preliminary systems tests were run for the purpose of determining concept feasibility. For convenience, the thruster was started and operated with the conventional power processor. After stable thruster operation was achieved, the beam supply was switched over from the conventional supply to the unregulated solar array. In addition, the fixed beam current reference was switched to the maximum power tracker control circuit output reference. When maximum power operation was achieved, dynamic tests were run in which the beam reference and therefore array current were reduced by resetting the integrator in the maximum power tracker control circuitry. Other tests were run by varying the solar array incident light. Finally thruster arcs were induced and their effects noted.

RESULTS AND DISCUSSION

Closed loop maximum power tracking was demonstrated with a 700 volt open circuit, 1.2 A short circuit current solar array supplying power for the thruster beam. Automatic maximum power tracking was established and maintained for a step change in the beam current reference and changes

in array incident light. In addition induced thruster arcs did not adversely affect power tracking.

System Response to Step Change in Beam

Current Reference

Figure 4 shows system parameter changes caused by a step change in the beam current reference. The initial operating condition is steady state operation at the maximum power point. The step reference change was introduced by rapidly resetting the integrator. At this time the main vaporizer turns full off in response to the new lowered reference. The power tracker now has no effect because the array current perturbing signal is cut off by this non-linear condition. It takes about 2 minutes for the thruster beam current to reach the new beam current reference and the power tracker to regain control. During this time the beam current reference stays constant. When the beam current reaches the reference point shown it is evident from the increasing beam current, increasing power and increasing beam current reference that the controller is starting to drive towards the maximum power point. It is also seen from figure 4 that the phase demodulator output averages a positive value. This positive value continues to drive the integrator towards the maximum power point. Furthermore, the first derivative is essentially in phase with the clock until the maximum power point is again reached. The recurring low amplitude distortions in the first derivative of power with a period of approximately seven seconds are caused by interactions between the thruster main vaporizer and cathode vaporizer control loops. The oscillations are also evident when the array and maximum power tracker are not in use. The interactions occur because the power console used has not been modified to contain the necessary compensation for this particular thruster. The latest 30-cm thruster control loop compensation methods are discussed in reference 18. The power versus time record shows that the power recovers to its maximum after a step change in the beam current reference.

System Response to Increase Array Incident Light

Figure 5 shows the system response to a step increase in incident light in one of the five modules. First one of the array module lamp power supplies was set at 80 volts. When maximum power point operation was established, the lamp power supply voltage was increased to 120 volts. It is seen from the power versus time recording that a new higher power level was reached and maintained. This step increase in incident light caused the initial operating point to be on the low current side of the maximum power point. The effect is similar to reducing the current reference.

System Response to Decrease in Array incident Light

Figure 6 shows system response to a step decrease in incident light. One of the five array module lamp power supplies was set at 115 volts. When maximum power operation was achieved, the lamp power supply voltage was lowered to 105 volts. This forced the system into operation on the high current side of the maximum power point. After the step change it is seen from the power versus time record in figure 6 that a new, lower maximum power point is reached.

In general, the array voltage decreases very rapidly with increasing array current on the high current side of the maximum power point. In addition the thruster tends to arc at very low array voltages so large changes in array current on the high current side of the maximum power point were avoided during this test. A change from 120 volts to 80 volts (not shown in the Figures) on one of the solar array module lamp power supplies caused the thruster to arc. No effort was made in these preliminary tests to find the largest step change that the system would tolerate without thruster arcing. However, a circuit was later added that would reset the integrator a fixed amount for each thruster arc, should the step reduction in incident light be larger enough to be outside the control range. This circuit is shown in the appendix.

System Response to Thruster Short Circuits

Thruster arcs were induced by turning off the accelerator power supply. Figure 7 shows the system during and recovering from thruster arcs. It is evident from the power versus time record that the system maintained control at the maximum power point. This noise immunity is due to the slow response of the control circuits and to filtering and shielding precautions.

General Comments

All the tests were run without filters across the array. However, if the thruster beam current has a high noise component caused by the thruster, filters may be needed for EMI Control. The filters should not adversely affect the maximum power tracking function. In fact, filters are desirable to reduce array excursions due to thruster noise to a minimum. High level noise induced excursions in beam voltage and current will result in a net power into the thruster that averages less than the array power available. This is simply because the operating point on the array characteristic varies around the maximum power point. For all of these initial tests, the control circuit time constants and the perturbing signal amplitudes were not optimized over the range of power levels. However, it is judged that this system is inherently capable of operation over a wide power range. In addition, if only a low voltage solar array can be used, then this system approach is judged to be viable for systems using an unregulated voltage step-up power supply between the array and the thruster beam. Furthermore if needed, multi-thruster operation should be possible. All thruster beam loads could be controlled from the same reference or some thrusters could be full on while one or more others are adjusted to maximize use of solar array power.

It is also judged that maximum thrust could be approximately tracked with this control scheme. This would be accomplished by replacing the array voltage input with a circuit that takes the square root of voltage. The system would then maximize the function for thrust:

$$T(\text{mN}) = 2.039 I_A \sqrt{V_A}$$

CONCLUSIONS

A new solar array/ion thruster system control concept has been developed and demonstrated. An ion thruster beam load is used to automatically and continuously operate an unregulated solar array at its maximum power point. The same control technique could be used if an intervening unregulated power supply were used to accommodate a lower array voltage. Furthermore, multithruster operation is judged possible. The benefit of using this control technique is that the mass-to-power ratio of the system could be minimized and the system hardware simplified. From a mission analysis viewpoint there is added complexity since the specific impulse and thrust vary according to the solar array temperature, incident light and degradation for a specific mission. The cost of implementing this control system would be small; only a small number of low level control circuits are required. It is estimated that a well-designed flight-type control system would comprise less than 100 components and would dissipate less than 1 watt. Since the system is closed loop, it is judged that the array maximum power could be tracked to within 1 percent. Control is ultimately limited by the need to perturb array power. The control system is capable of operation over all useful ranges of thruster beam voltage and current without adjustments. System response time is ultimately limited by the thruster main vaporizer control loop, which is dominated by a thermal time constant.

It is also judged that approximate operation at the maximum thrust point is possible with this system. This would be accomplished by replacing the voltage sensing input by a circuit that takes the square root of voltage. The system then maximizes the approximate equation for thrust:

$$T(\text{mN}) \cong 2.039 I_A \sqrt{V_A}$$

APPENDIX - MAXIMUM POWER TRACKER CONTROL CIRCUITS

The control circuits were developed primarily for the purpose of demonstrating the control concept. Filtering and shielding were deliberately over designed to minimize the time for initial design and debugging. Figure 8 is a schematic diagram and parts list of the maximum power tracker control circuits used. The figure shows essentially the circuits used for the tests except for minor changes made after the test for operational convenience. Q1 and U1 in Figure 8 form the transconductance multiplier shown functionally in figure 3. Amplifier U2 is the differentiator, U3 the zero crossing detector and shaping circuit. U4 and U5 together with U6 and Q2 comprise the phase demodulator and provide ground isolation if needed. U10 is the integrator and U11 is the summing amplifier that provides the beam current reference.

The perturbing ramp is generated by C42, R47 and R44. An external reset circuit was added after the tests reported herein. It is formed from Q3, Q4, and U9. Lamps L1 and L2 are used to provide a visual indication of the first derivative and clock phase. U7 and U8 form the clock.

A flight type version of this circuit would require the use of full temperature range components as well as the use of flight standard parts. Furthermore several possibilities for component parts count reduction could be explored.

REFERENCES

1. Atkins, K. L.: Mission Applications of Electric Propulsion. AIAA Paper 74-1085, Oct. 1974.
2. Duxbury, J. H.; and Finke, R. C.: A Candidate Mission Using the Shuttle and Solar Electric Propulsion. AAS Paper 75-163, 1975.
3. Guttman, C. H.; et al.: The Solar Electric Propulsion Stage Concept for High Energy Missions. AIAA Paper 72-465, Apr. 1972.
4. Sauer, C. G., Jr.: Trajectory Analysis and Performance for SEP Comet Encke Mission. AIAA Paper 73-1059, Oct. 1973.
5. Payload Utilization of SEPS. Rept. D-180-19783-1, Boeing Aerospace Co., 1976.
6. Concept Definition and Systems Analysis Study for a Solar Electric Propulsion Stage. Rept. SD74-SA-0176-1, Rockwell International, 1975.
7. Stearns, J. W.: Large-Payload Earth-Orbit Transportation With Electric Propulsion. (JPL-TM-33-793, Jet Propulsion Lab.; NAS 7-100), NASA CR-148973, 1976.
8. Schnelker, D. E.; and Collett, C. R.: 30-cm Engineering Model Thruster Design and Qualification Tests. AIAA Paper 75-341, Mar. 1975.
9. Triner, James E.: A Digital Regulated Solar Array Power Module. NASA TM X-2314, 1971.
10. Gooder, Suzanne T.: Series-Parallel Method of Direct Solar Array Regulation. NASA TM X-73505, 1976.
11. Gooder, Suzanne T.: Evaluation of 30 cm Ion Thruster Operational Compatibility With Integrally Regulated Solar Array Power Source. NASA TN D-8428, 1977.
12. Gruber, Robert: High Efficiency Solar Cell Array Peak Power Tracker and Battery Charger. IEEE Power Conditioning Specialists Conference. Inst. Electr. Electron Eng., Inc., 1970, pp. 128-138.

13. Paulkovich, John; and Rodriguez, G. E.: Maximum Power Transfer by Conductance Comparison. IEEE Power Conditioning Specialists Conference. Inst. Electr. Electron Eng., Inc., 1970, pp. 114-127.
14. Advanced Voltage Regulator Techniques as Applied to Maximum Power Point Tracking for the NIMBUS Meteorological Satellite. (AED-R-3221, Radio Corp. of Am.; NAS5-3248), NASA CR-93413, 1967.
15. Gardner, J. A.: Solar Electric Propulsion System Integration Technology (SEPSIT). Volume 1: Technical Summary. (JPL-TM-33-583-Vol-1, Jet Propulsion Lab.; NAS7-100), NASA CR-130701, 1972.

Gardner, J. A.: Solar Electric Propulsion System Integration Technology (SEPSIT). Volume 2: Encke Rendezvous Mission and Space Vehicle Functional Description. (JPL-TM-33-583-Vol-2, Jet Propulsion Lab.; NAS7-100), NASA CR-130702, 1972.

Gardner, J. A.: Solar Electric Propulsion System Integration Technology (SEPSIT). Volume 3: Supporting Analyses. (JPL-TM-33-583-Vol-3, Jet Propulsion Lab.; NAS7-100), NASA CR-130703, 1972.
16. Sovey, J. S.; and King, H. J.: Status of 30-cm Mercury Ion Thruster Development. AIAA Paper 74-1117, Oct. 1974.
17. Kolecki, Joseph C.; and Gooder, Suzanne T.: Laboratory 15 kV High Voltage Solar Array Facility. NASA TM X-71860, 1976.
18. Collett, C.: Thruster Endurance Test. (Hughes Research Labs.; NAS3-15523), NASA CR-135011, 1976.
19. Robson, R. R.: Compensated Control Loops For a 30-cm Ion Thruster. AIAA Paper 76-994, Nov. 1976.

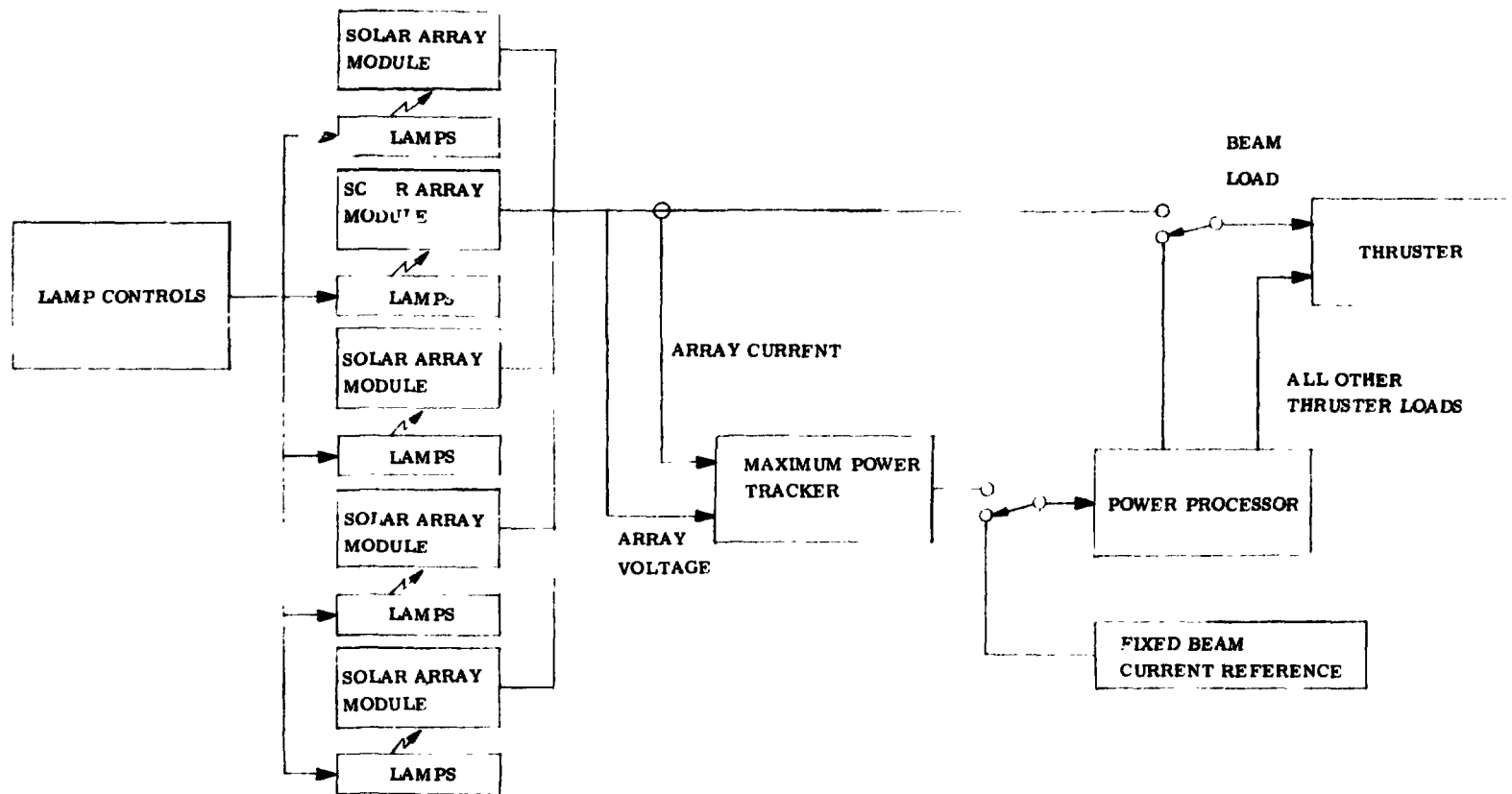


FIGURE 1. - FUNCTIONAL DIAGRAM OF TEST CONFIGURATION

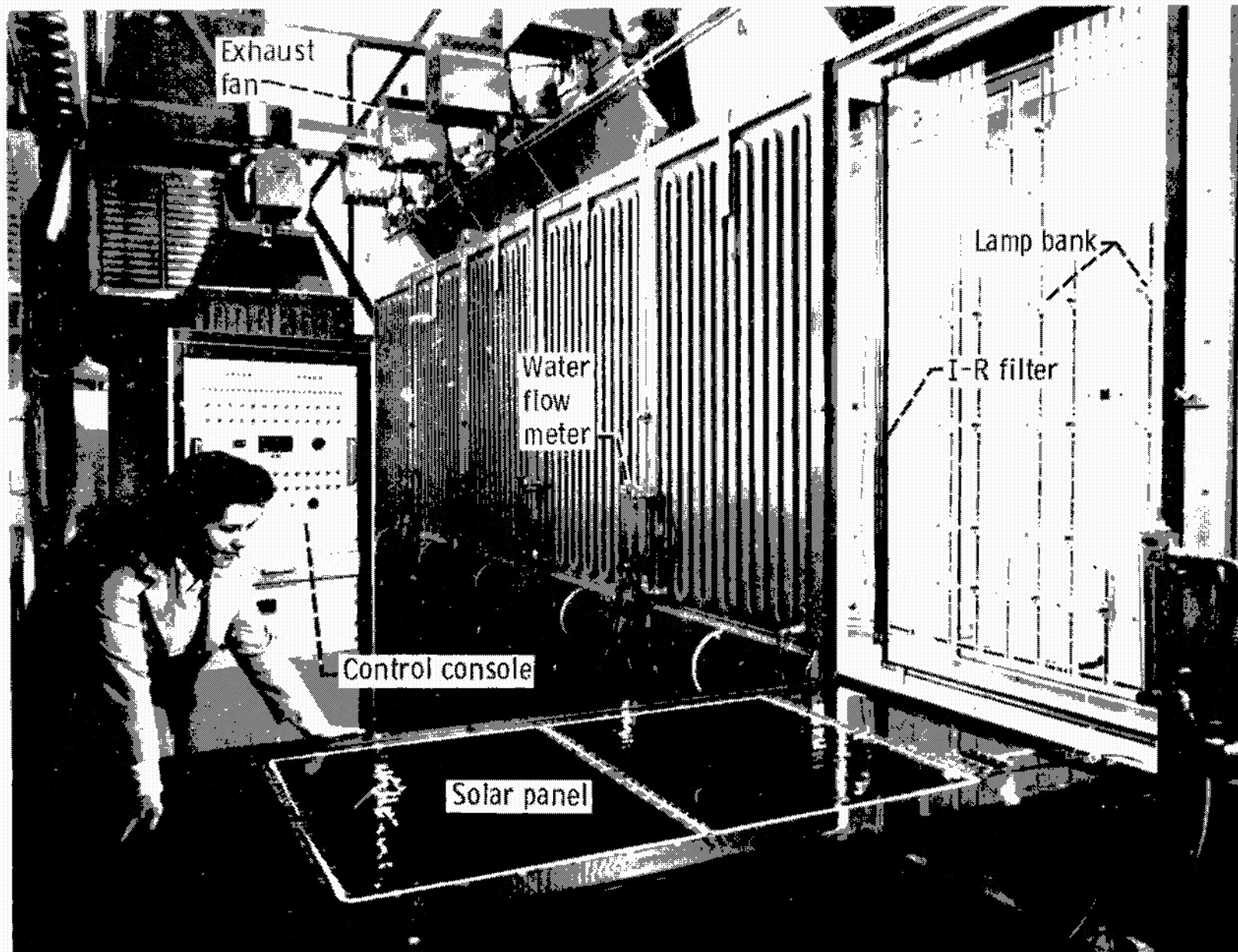
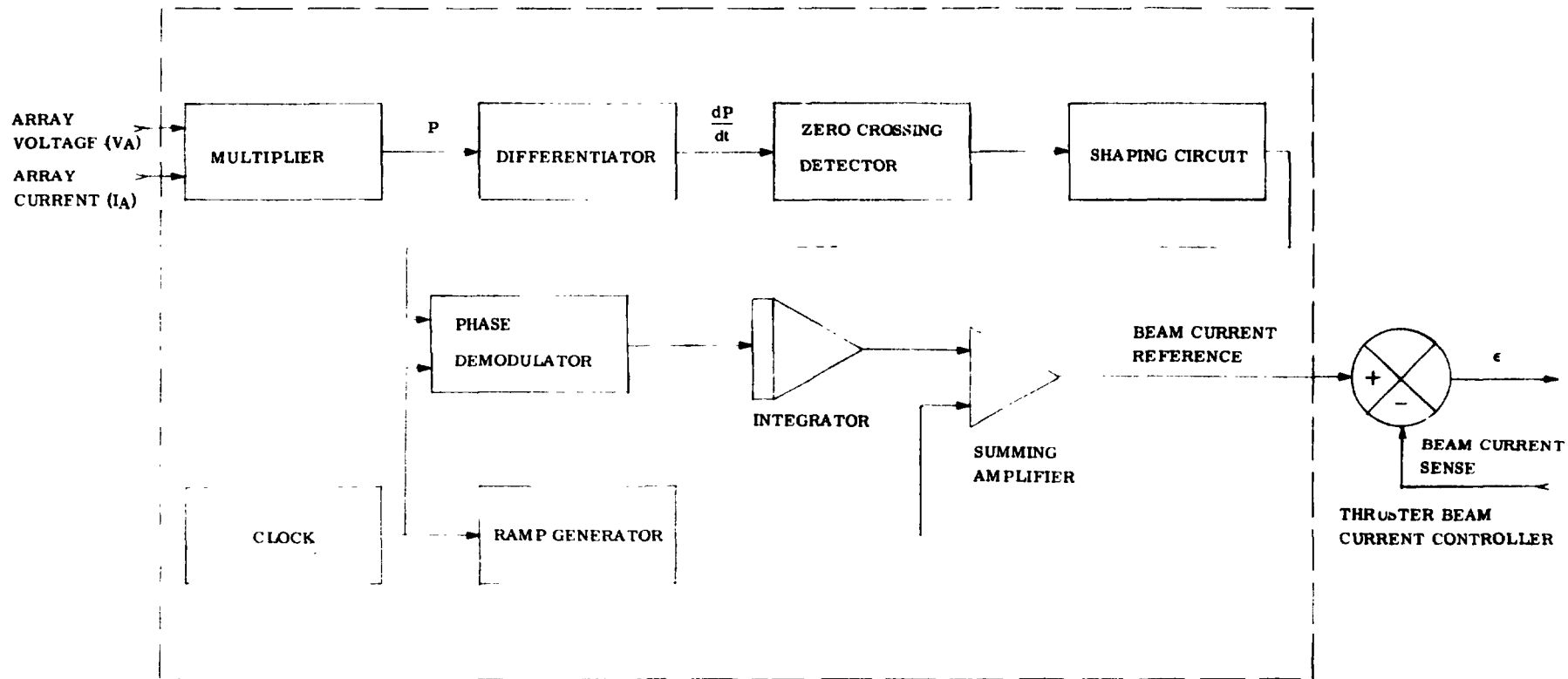


Figure 2. - 1-Kilowatt laboratory solar array facility with one of the nine modules opened to display array panel and lamp bank.



**FIGURE 3. - FUNCTIONAL DIAGRAM
 SOLAR ARRAY/ION THRUSTER MAXIMUM
 POWER TRACKER CONTROL CIRCUIT**

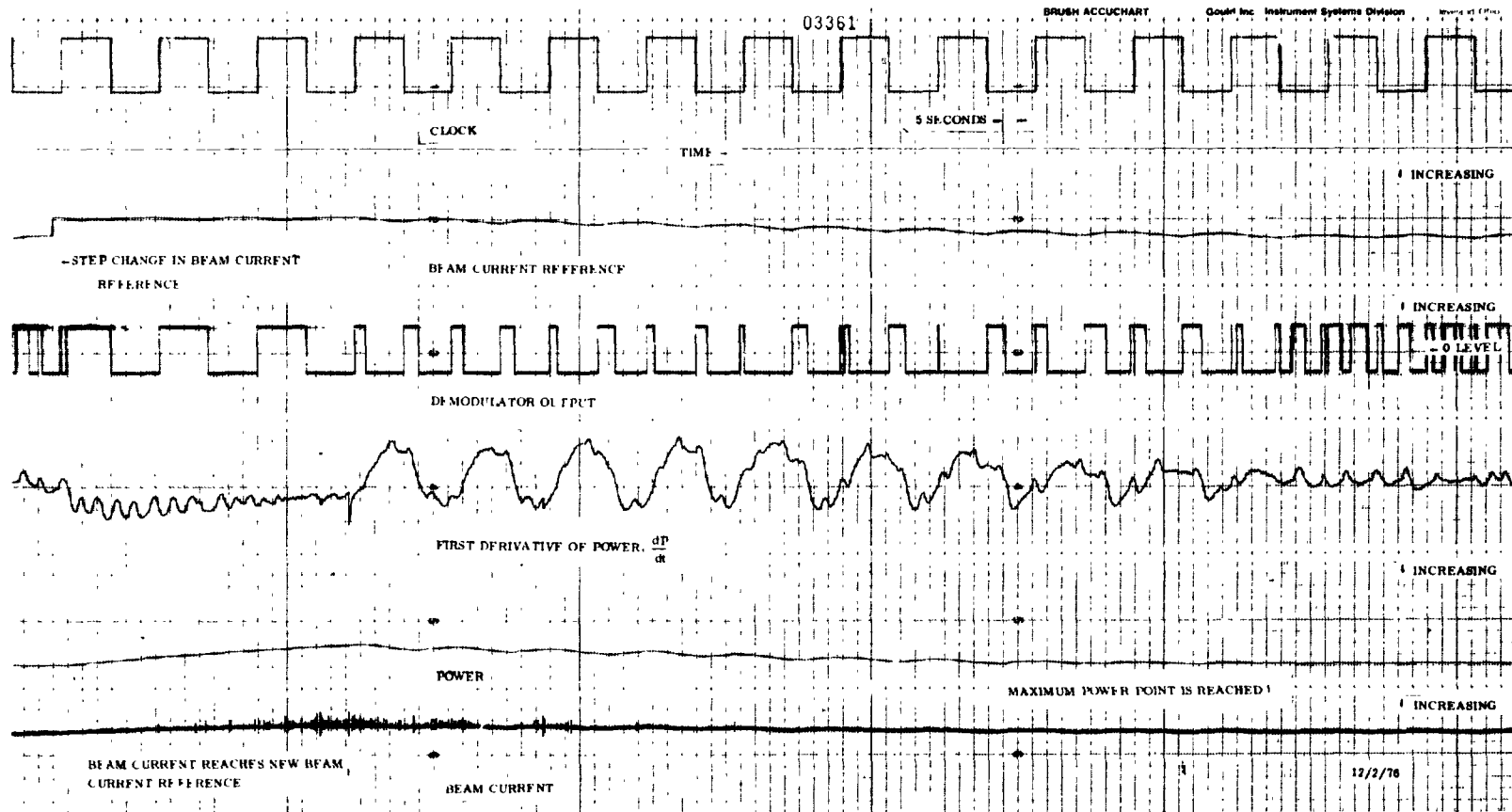


FIGURE 4 - SYSTEM RESPONSE TO A STEP CHANGE IN BEAM CURRENT REFERENCE.

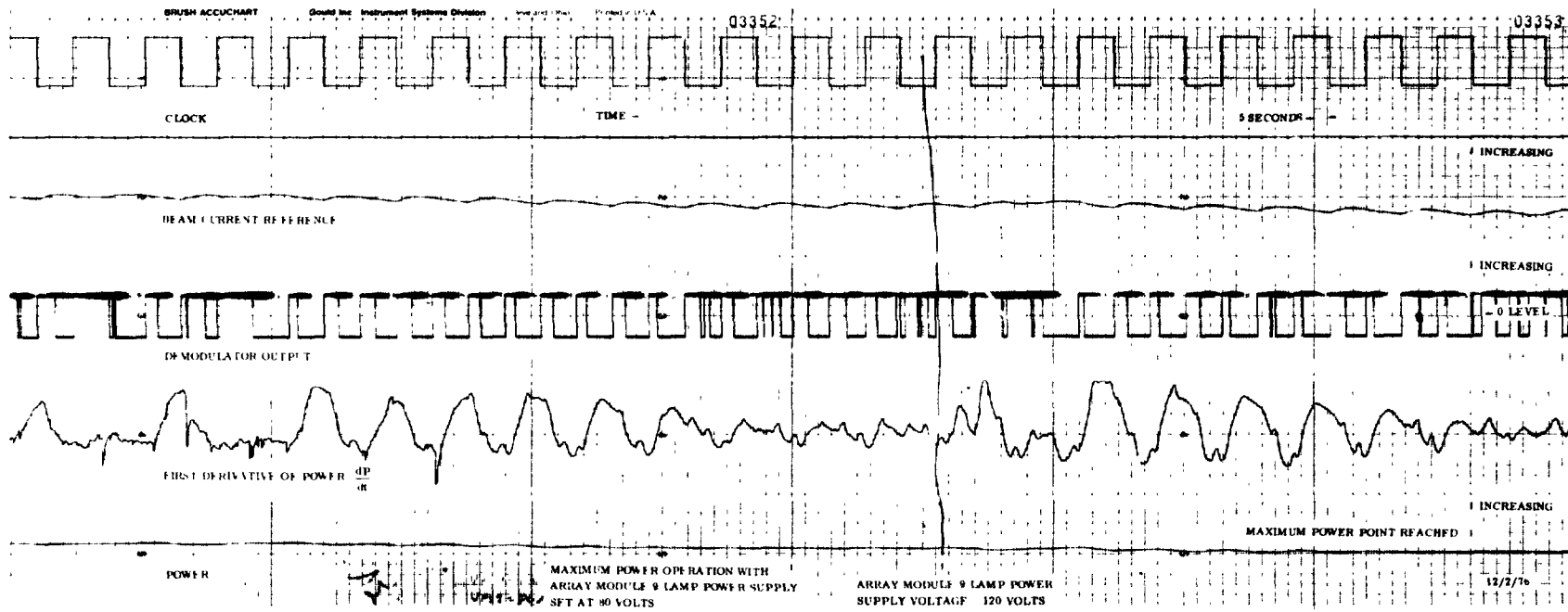


FIGURE 5 - SYSTEM RESPONSE TO INCREASE IN ARRAY INCIDENT LIGHT.

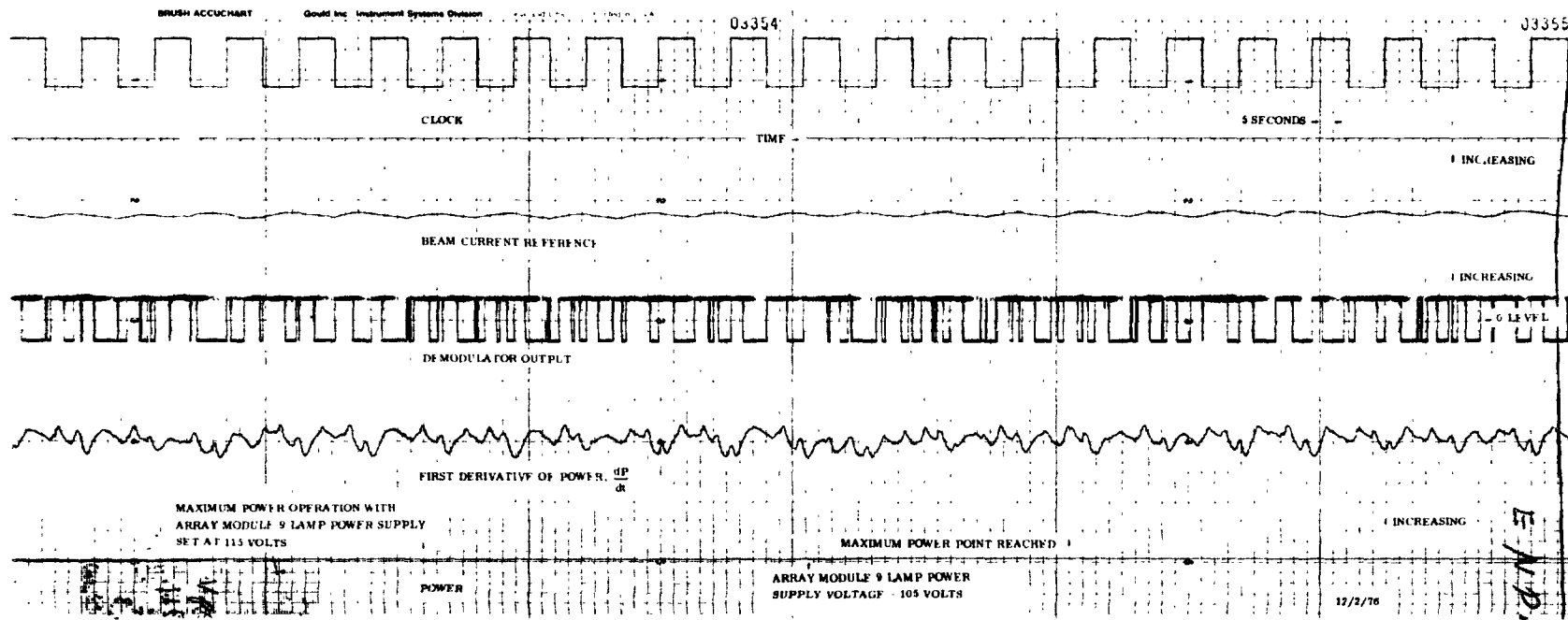
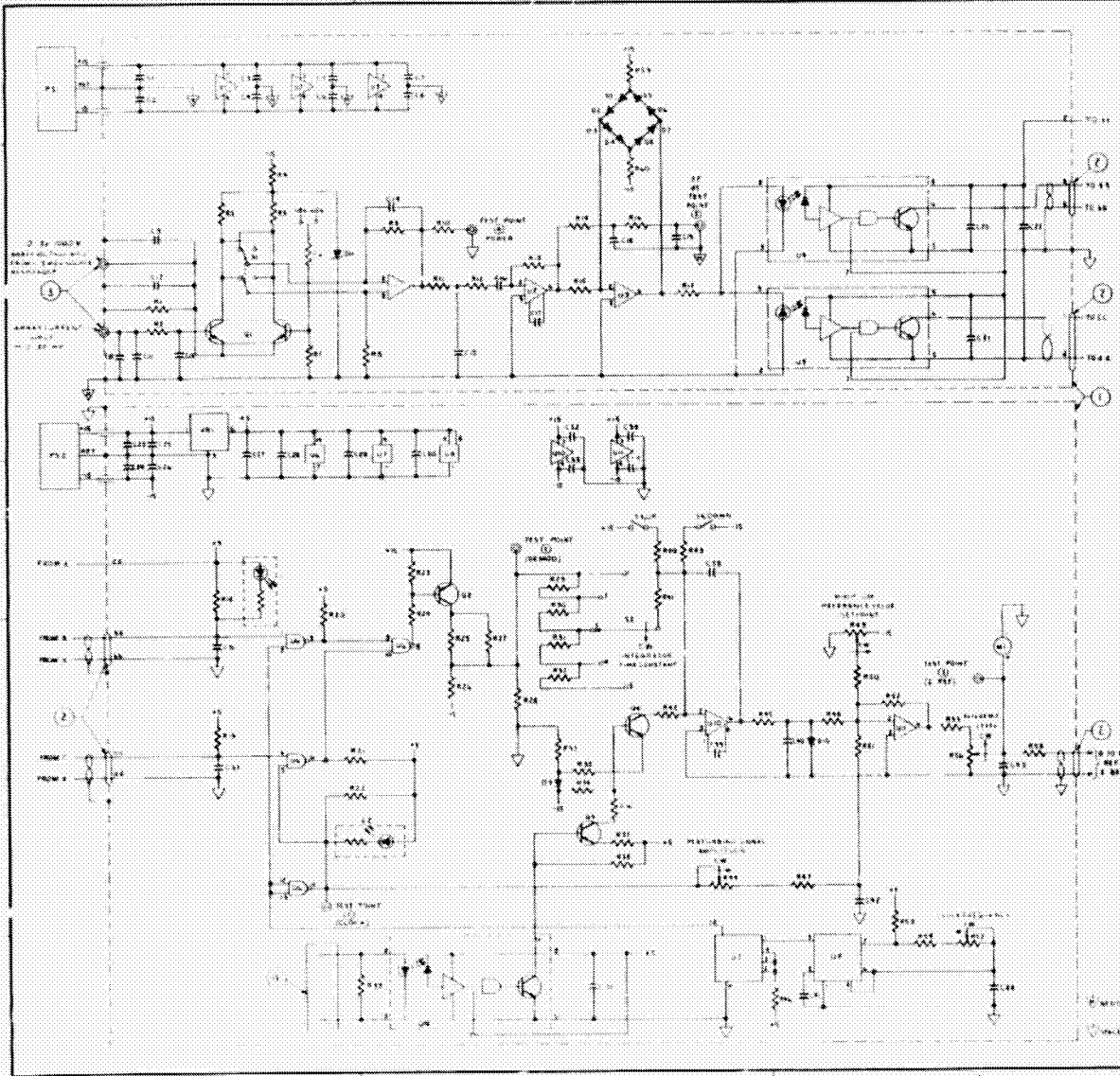


FIGURE 6 - SYSTEM RESPONSE TO DECREASE IN ARRAY INCIDENT LIGHT.



FIGURE 7 - SYSTEM RESPONSE TO THRUSTER BEAM ARCS.



PARTS LIST		QTY
ITEM	DESCRIPTION	
100	CAPACITOR 100P	1
101	CAPACITOR 100P	1
102	CAPACITOR 100P	1
103	CAPACITOR 100P	1
104	CAPACITOR 100P	1
105	CAPACITOR 100P	1
106	CAPACITOR 100P	1
107	CAPACITOR 100P	1
108	CAPACITOR 100P	1
109	CAPACITOR 100P	1
110	CAPACITOR 100P	1
111	CAPACITOR 100P	1
112	CAPACITOR 100P	1
113	CAPACITOR 100P	1
114	CAPACITOR 100P	1
115	CAPACITOR 100P	1
116	CAPACITOR 100P	1
117	CAPACITOR 100P	1
118	CAPACITOR 100P	1
119	CAPACITOR 100P	1
120	CAPACITOR 100P	1
121	CAPACITOR 100P	1
122	CAPACITOR 100P	1
123	CAPACITOR 100P	1
124	CAPACITOR 100P	1
125	CAPACITOR 100P	1
126	CAPACITOR 100P	1
127	CAPACITOR 100P	1
128	CAPACITOR 100P	1
129	CAPACITOR 100P	1
130	CAPACITOR 100P	1
131	CAPACITOR 100P	1
132	CAPACITOR 100P	1
133	CAPACITOR 100P	1
134	CAPACITOR 100P	1
135	CAPACITOR 100P	1
136	CAPACITOR 100P	1
137	CAPACITOR 100P	1
138	CAPACITOR 100P	1
139	CAPACITOR 100P	1
140	CAPACITOR 100P	1
141	CAPACITOR 100P	1
142	CAPACITOR 100P	1
143	CAPACITOR 100P	1
144	CAPACITOR 100P	1
145	CAPACITOR 100P	1
146	CAPACITOR 100P	1
147	CAPACITOR 100P	1
148	CAPACITOR 100P	1
149	CAPACITOR 100P	1
150	CAPACITOR 100P	1
151	CAPACITOR 100P	1
152	CAPACITOR 100P	1
153	CAPACITOR 100P	1
154	CAPACITOR 100P	1
155	CAPACITOR 100P	1
156	CAPACITOR 100P	1
157	CAPACITOR 100P	1
158	CAPACITOR 100P	1
159	CAPACITOR 100P	1
160	CAPACITOR 100P	1
161	CAPACITOR 100P	1
162	CAPACITOR 100P	1
163	CAPACITOR 100P	1
164	CAPACITOR 100P	1
165	CAPACITOR 100P	1
166	CAPACITOR 100P	1
167	CAPACITOR 100P	1
168	CAPACITOR 100P	1
169	CAPACITOR 100P	1
170	CAPACITOR 100P	1
171	CAPACITOR 100P	1
172	CAPACITOR 100P	1
173	CAPACITOR 100P	1
174	CAPACITOR 100P	1
175	CAPACITOR 100P	1
176	CAPACITOR 100P	1
177	CAPACITOR 100P	1
178	CAPACITOR 100P	1
179	CAPACITOR 100P	1
180	CAPACITOR 100P	1
181	CAPACITOR 100P	1
182	CAPACITOR 100P	1
183	CAPACITOR 100P	1
184	CAPACITOR 100P	1
185	CAPACITOR 100P	1
186	CAPACITOR 100P	1
187	CAPACITOR 100P	1
188	CAPACITOR 100P	1
189	CAPACITOR 100P	1
190	CAPACITOR 100P	1
191	CAPACITOR 100P	1
192	CAPACITOR 100P	1
193	CAPACITOR 100P	1
194	CAPACITOR 100P	1
195	CAPACITOR 100P	1
196	CAPACITOR 100P	1
197	CAPACITOR 100P	1
198	CAPACITOR 100P	1
199	CAPACITOR 100P	1
200	CAPACITOR 100P	1

GENERAL NOTES

UNLESS OTHERWISE NOTED ALL CAPACITORS ARE 50V. CAP. CO. IS IN FORM. ALL CAPACITORS ARE 50V.

NOTE: IN PLACEMENT OF ALL CAPACITORS, VALUES FOR 100P MUST BE 100P. CAPACITORS 100P MUST BE 100P. CAPACITORS 100P MUST BE 100P.

ALL TEST POINTS ARE TO BEAL CONNECTORS.

ITEM	DESCRIPTION	QTY
100	CAPACITOR 100P	1
101	CAPACITOR 100P	1
102	CAPACITOR 100P	1
103	CAPACITOR 100P	1
104	CAPACITOR 100P	1
105	CAPACITOR 100P	1
106	CAPACITOR 100P	1
107	CAPACITOR 100P	1
108	CAPACITOR 100P	1
109	CAPACITOR 100P	1
110	CAPACITOR 100P	1
111	CAPACITOR 100P	1
112	CAPACITOR 100P	1
113	CAPACITOR 100P	1
114	CAPACITOR 100P	1
115	CAPACITOR 100P	1
116	CAPACITOR 100P	1
117	CAPACITOR 100P	1
118	CAPACITOR 100P	1
119	CAPACITOR 100P	1
120	CAPACITOR 100P	1
121	CAPACITOR 100P	1
122	CAPACITOR 100P	1
123	CAPACITOR 100P	1
124	CAPACITOR 100P	1
125	CAPACITOR 100P	1
126	CAPACITOR 100P	1
127	CAPACITOR 100P	1
128	CAPACITOR 100P	1
129	CAPACITOR 100P	1
130	CAPACITOR 100P	1
131	CAPACITOR 100P	1
132	CAPACITOR 100P	1
133	CAPACITOR 100P	1
134	CAPACITOR 100P	1
135	CAPACITOR 100P	1
136	CAPACITOR 100P	1
137	CAPACITOR 100P	1
138	CAPACITOR 100P	1
139	CAPACITOR 100P	1
140	CAPACITOR 100P	1
141	CAPACITOR 100P	1
142	CAPACITOR 100P	1
143	CAPACITOR 100P	1
144	CAPACITOR 100P	1
145	CAPACITOR 100P	1
146	CAPACITOR 100P	1
147	CAPACITOR 100P	1
148	CAPACITOR 100P	1
149	CAPACITOR 100P	1
150	CAPACITOR 100P	1
151	CAPACITOR 100P	1
152	CAPACITOR 100P	1
153	CAPACITOR 100P	1
154	CAPACITOR 100P	1
155	CAPACITOR 100P	1
156	CAPACITOR 100P	1
157	CAPACITOR 100P	1
158	CAPACITOR 100P	1
159	CAPACITOR 100P	1
160	CAPACITOR 100P	1
161	CAPACITOR 100P	1
162	CAPACITOR 100P	1
163	CAPACITOR 100P	1
164	CAPACITOR 100P	1
165	CAPACITOR 100P	1
166	CAPACITOR 100P	1
167	CAPACITOR 100P	1
168	CAPACITOR 100P	1
169	CAPACITOR 100P	1
170	CAPACITOR 100P	1
171	CAPACITOR 100P	1
172	CAPACITOR 100P	1
173	CAPACITOR 100P	1
174	CAPACITOR 100P	1
175	CAPACITOR 100P	1
176	CAPACITOR 100P	1
177	CAPACITOR 100P	1
178	CAPACITOR 100P	1
179	CAPACITOR 100P	1
180	CAPACITOR 100P	1
181	CAPACITOR 100P	1
182	CAPACITOR 100P	1
183	CAPACITOR 100P	1
184	CAPACITOR 100P	1
185	CAPACITOR 100P	1
186	CAPACITOR 100P	1
187	CAPACITOR 100P	1
188	CAPACITOR 100P	1
189	CAPACITOR 100P	1
190	CAPACITOR 100P	1
191	CAPACITOR 100P	1
192	CAPACITOR 100P	1
193	CAPACITOR 100P	1
194	CAPACITOR 100P	1
195	CAPACITOR 100P	1
196	CAPACITOR 100P	1
197	CAPACITOR 100P	1
198	CAPACITOR 100P	1
199	CAPACITOR 100P	1
200	CAPACITOR 100P	1

FIGURE 1. RADIO RECEIVER RECEIVER SECTION (PARTIAL)

CFR 18123